Journal Name

ARTICLE

NIR Mechanochromic Behaviours of Tetracyanoethylene-Bridged Hexa-*peri*-Hexabenzocoronene Dimer and Trimer through Dissociation of C–C Bonds

Received 00th January 20xx,
Accepted 00th January 20xx

DOI: 10.1039/x0xx00000x

www.rsc.org/

Kazuma Oda, Satoru Hiroto* and Hiroshi Shinokubo*

Oxidation of dicyanomethyl-substituted hexa-*peri*-hexabenzocoronenes (HBCs) furnished tetracyanoethylene-bridged HBC dimer and trimer. The solid state structures of the oligomers were elucidated by single crystal X-ray diffraction analysis. In the solution state, these HBC oligomers exhibited conformational isomerism, depending on solvents and temperatures. Moreover, solid samples of the HBC dimer and trimer exhibited mechanochromism, showing near IR absorption upon grinding through generation of radical species. The formed radical was stable for 4 months, indicating persistent nature of the radical species. These NIR mechanochromic behaviours of HBC oligomers were originated from reversible C–C bond dissociation and formation of the tetracyanoethylene linkage between the HBC units.

Introduction

Mechanochromism is phenomena in which solid colour or luminescence colour changes by an external mechanical stimuli such as grinding,[1] pressing[2] and stretching.[3,4] Mechanochromic molecules have attracted significant attention as sensor, security ink, storage and biological application.[1b,5] Mechanochromic behaviours are originated from reversible changes in the states of materials, associated with π–π stacking,[6] CH–π interaction,[1a] hydrogen bonding,[2] metal–metal interaction,[7] conformation,[8] crystalline phase[9] and covalent bonds.[1b,4d,10]

Among various types of mechanochromism, bond dissociation-based mechanochromic molecules usually shows large chromic shift due to the formation of radical species. Some of congested 1,2-diarylethanes exhibit mechanochromism through reversible bond dissociation and formation involving stabilised benzyl radicals (Fig. 1). Lactone-based carbon-centred radicals **D** are not reactive toward dioxygen due to resonance stabilisation, allowing selective dimerisation.[11] Recently, Sakamaki, Seki and co-workers have reported mechanochromic behaviour of *para*-substituted aryldicyanomethyl dimers **E**.[12] In this mechanochromic process, the stability of phenyldicyanomethyl radical is a key factor, which dimerises to 1,2-diphenyl-1,1,2,2,-tetracyanoethane.[13]

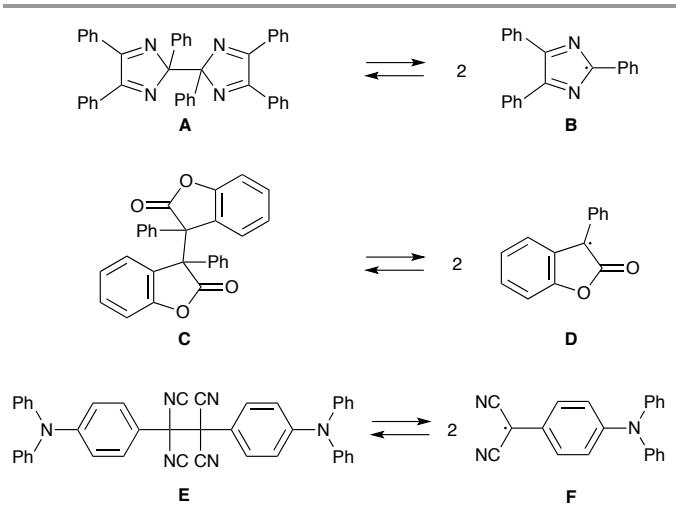

Fig. 1 Representative carbon-centred radicals exhibiting mechanochromic behaviour.

Hexa-*peri*-hexabenzocoronenes (HBCs) have received much attention as a motif in supramolecular assemblies and discotic liquid crystals because of their disc-like shapes and large π-conjugation systems.[14] We have recently reported regioselective functionalisations of HBCs through iridium catalysed direct C–H borylation, enabling facile installation of various substituents to HBCs.[15] We anticipated that an HBC-substituted dicyanomethyl radical would exhibit enhanced stability because of significant spin delocalisation over the large π-conjugation system of the HBC unit.[16]

Here we report the synthesis and oxidation behaviour of HBCs containing one and two dicyanomethyl groups. Mono- and disubstituted HBCs were oxidised to afford tetracyanoethylene-linked dimer and trimer, respectively. In addition, these oligomers exhibited distinct mechanochromism

[a] *Department of Molecular and Macromolecular Chemistry, Graduate School of Engineering, Nagoya University, Aichi, 464-8603, Japan. E-mail: hshino@chembio.nagoya-u.ac.jp, hiroto@chembio.nagoya-u.ac.jp; Fax: (+81)-52-789-5113*

Electronic Supplementary Information (ESI) available: ^{1}H NMR and ^{13}C NMR spectra for all compounds, optical properties of **2** and **6**, X-ray crystal structure of **6** and theoretical calculations. See DOI: 10.1039/x0xx00000x

in the solid state due to reversible C–C bond dissociation and formation. Grinding of the solid samples of the oligomers generated the persistent radical species under aerobic conditions, which showed intense NIR absorption bands.

Results and Discussion

Dicyanoethylene-bridged HBC dimer **2** was prepared through oxidation of **1** with an excess amount of PbO_2 according to the previous report (Scheme 1).[17] The ^{1}H NMR spectrum of **2** exhibited two sharp peaks at 9.03 and 7.08 ppm and a broad peak at 7.03 ppm at room temperature in $CDCl_3$. The structure of **2** was unambiguously determined by X-ray diffraction analysis.[18] Two HBC units were bridged by a tetracyanoethylene group, in which two HBC moieties aligned in the same direction, *gauche*-form (Fig. 2). Notably, the bond length of the central carbon–carbon bond on the tetracyanoethylene unit of **2** was 1.610(7) Å, which is remarkably longer than a typical sp^3–sp^3 C–C bond length (1.54 Å).

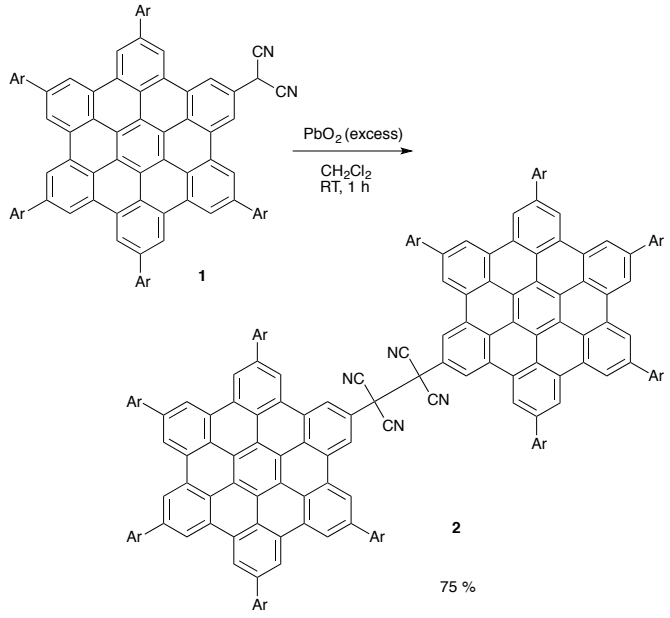

Scheme 1. Synthesis of dicyanoethylene-bridged HBC dimer **2**.

The ^{1}H NMR spectrum of **2** exhibited two sharp peaks at 9.03 and 7.08 ppm and a broad peak at 7.03 ppm at room temperature in $CDCl_3$. The structure of **2** was unambiguously determined by X-ray diffraction analysis.[17] Two HBC units were bridged by a tetracyanoethylene group, in which two HBC moieties aligned in the same direction, *gauche*-form (Fig. 2). Notably, the bond length of the central carbon–carbon bond on the tetracyanoethylene unit of **2** was 1.610(7) Å, which is remarkably longer than a typical sp^3–sp^3 C–C bond length (1.54 Å).

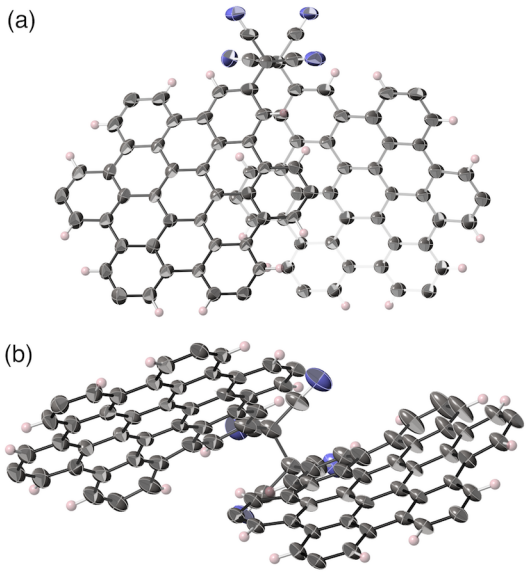

Fig. 2 X-ray crystal structure of **2**. (a) Top view and (b) side view. Mesityl groups were omitted for clarity. The thermal ellipsoids were scaled at the 50% probability level.

To further analyse the conformation of **2** in solution, variable temperature (VT) ^{1}H NMR analysis was performed in various solvents. In THF-d_8, new sharp peaks appeared from 5 to 10 ppm as the temperature decreased (Fig. S6). At –60 °C, mesityl proton peaks at 6.40 and 5.26 ppm and a methyl proton peak at –0.12 ppm showed upfield shift because of the ring current effect by the HBC unit (Fig. S6c). In the DOSY NMR spectrum at –60 °C in THF-d_8, the peaks around 7.0 and 9.5 ppm have larger diffusion constants (D) than other peaks (Fig. S7).[19] These results indicated that two different conformers of **2** exist and the appearance of new peaks can be attributed to suppression of interconversion between two conformers at low temperature.[10b] Restricted rotation around the central C–C bond due to steric hindrance of the substituents provides two rotamers; *anti*-form in which two HBC units align in the opposite direction and *gauche*-form in which two HBC units point in the same directions (Scheme 2). Upfield-shifted signals were characterised as protons of the *gauche*-form, while peaks at 7.0 and 9.5 ppm was assigned as protons of the centrosymmetric *anti*-form. The ratio of these isomers at –60 °C was determined to be *gauche*:*anti* = 71:29 on the basis of the ^{1}H NMR spectrum in THF-d_8. On the other hand, six HBC proton peaks around 9 ppm and three mesityl peaks around 7 ppm were intensified at higher temperatures in 1,1,2,2-tetrachloroethane-d_2 (Fig. S8). This result suggests that interconversion between two rotamers is facilitated at high temperatures.

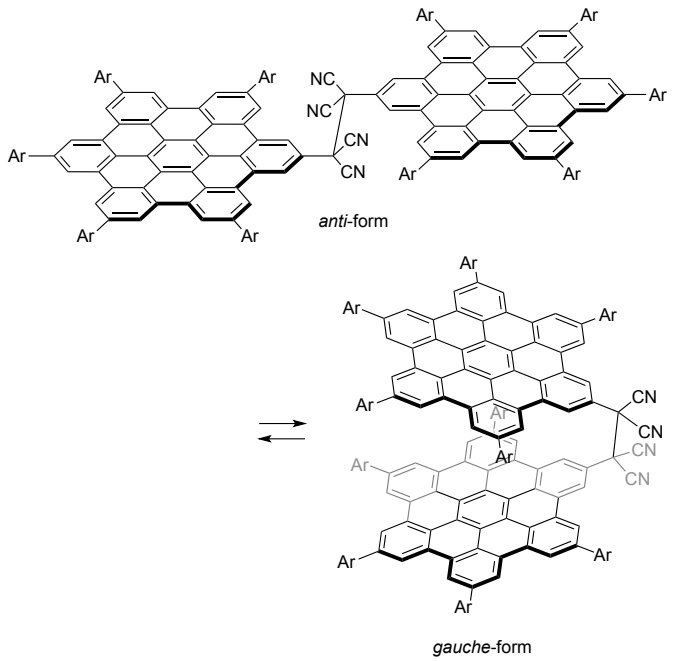

Scheme 2. Schematic views of thermal interconversion between *anti*-form and *gauche*-form of **2**.

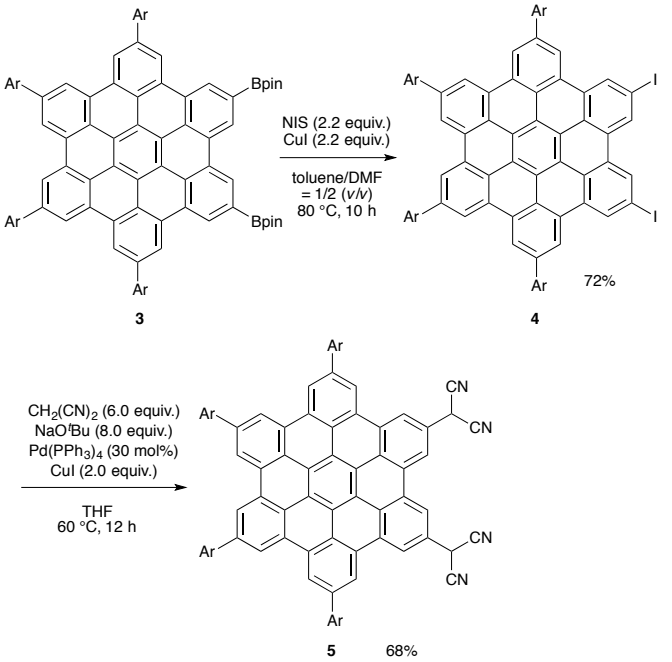

Scheme 3. Synthesis of 2,5-bis(dicyanomethyl) HBC **5**.

The structures of **2** were fully optimised by theoretical calculations (Fig. S20). The zero-point energy calculations of *anti*- and *gauche*-forms at the B3LYP/6-31+G(d)//ONIOM(B3LYP/6-31G(d):PM6 level revealed that the gauche-form is more stable than the *anti*-form by 2.7 kcal mol^{-1}, suggesting the dominance of the *gauche*-form in solution (Table S1). These results indicate the presence of dynamic conformational change of **2** in the solution state.

We expected that introduction of two dicyanomethyl groups would allow to construct cyclic oligomers. Scheme 3 depicts the preparation of 2,5-bis(dicyanomethyl)-substituted HBC **5**. Diborylated HBC **3** was converted to diiodo HBC **4** in 82% by treatment with copper(I) iodide (2.2 equiv) and *N*-iodosuccinimide (2.2 equiv) in a mixture of DMF/toluene (2:1, *v/v*). Dicyanomethyl HBC **5** was obtained in 68% via Takahashi coupling of **4** with malononitrile (6.0 equiv) in the presence of $Pd(PPh_3)_4$ (30 mol%), copper(I) iodide (2.0 equiv), and sodium *tert*-butoxide (8.0 equiv.) in THF. A singlet peak at 5.71 ppm in the ^{1}H NMR spectrum of **5** was assigned as methine protons, which were disappeared completely by the addition of potassium *tert*-butoxide (2.2 equiv) in THF-d_8 under argon atmosphere.

As in the case with the reaction of dicyanomethyl HBC **1**, oxidation of **5** with an excess amount of PbO_2 provided a non-fluorescent compound (Scheme 4). High-resolution mass analysis of this compound showed the parent ion peak at m/z = 3386.3363, which is consistent with the exact mass of tetracyanoethylene-bridged HBC trimer **6**. We found that the ^{1}H NMR spectrum of **6** was varied significantly in different solvents. The ^{1}H NMR spectra of **6** in dichlorobenzene-d_4, tetrachloroethane-d_2 and toluene-d_8 simply showed six HBC proton signals from 8 to 9 ppm and two mesityl peaks around 7 ppm (Fig. S9, S10, S12). On the other hand, multiple peaks are observed in the range of 5–11 ppm in tetrahydrofuran-d_8 (Fig. S13). In addition, the ^{1}H NMR spectra also depended on the measurement temperatures (Fig. S12, S14). These results indicated that HBC trimer **6** also showed dynamic behaviour involving at least two conformers in the solution state.

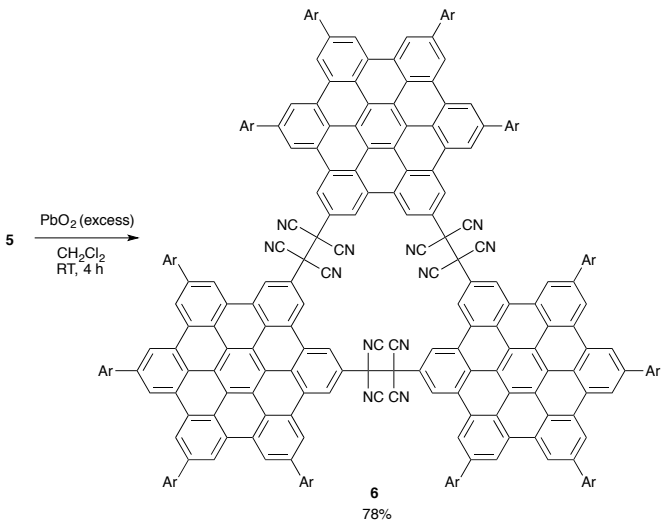

Scheme 4. Oxidation trimerisation of 2,5-bis(dicyanomethyl) HBC **6**.

Two geometries of trimer **6** were optimised by theoretical calculations (Fig. 3). The simple ^{1}H NMR peaks of **6** in tetrachloroethane-d_2 and in toluene-d_8 should be due to the D_3 symmetrical structure, *anti-anti-anti*-form (Fig. 3a). In contrast, the complicated ^{1}H NMR peaks of **6** in tetrahydrofuran-d_8 should be ascribed to the unsymmetrical structure, *anti-gauche-gauche*-form (Fig. 3b). The conformational change depending on solvents is probably caused by the lyophobic effect. The structure of **6** was elucidated by preliminary X-ray diffraction analysis (Fig. S20). In the structure of trimer **6**, three HBC units were connected with three tetracyanoethylene units. Two of bridged tetracyanoethylene units adopt *gauche*-type conformation, while another one has *anti*-type conformation (*anti-gauche-gauche*-form).

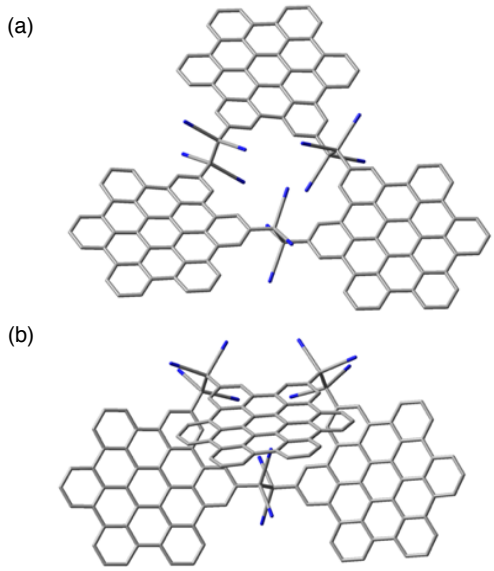

Fig. 3 Optimised geometries of trimer **6** for (a) D_3 symmetrical *anti-anti-anti*-form and (b) C_2 symmetrical *anti-gauche-gauche*-form. Mesityl groups were replaced with hydrogen to reduce calculation costs.

UV-vis absorption spectra of monomer **1**, **5**, dimer **2** and trimer **6** in dichloromethane are shown in Fig. 4. The lowest energy bands of dimer **2** (λ_{max} = 446 nm) and trimer **6** (λ_{max} = 445 nm) exhibited almost no change as compared with that of monomer **1** (λ_{max} = 444 nm) and **5** (λ_{max} = 445 nm), suggesting almost negligible electronic interactions between HBC units. Dimer **2** and trimer **6** exhibited no fluorescence in dichloromethane, indicating that the dynamic motions at flexible tetracyanoethylene linkages increase non-radiative decay in the singlet-excited states.

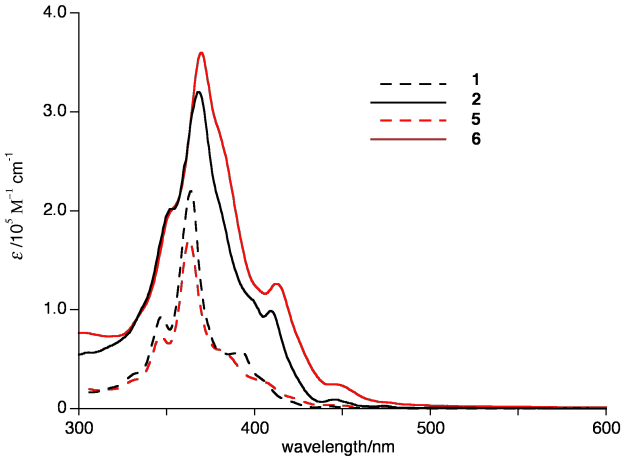

Fig. 4 UV-vis absorption spectra of **1**, **2**, **5** and **6** in dichloromethane.

Interestingly, solid colours of dimer **2** changed from yellow to brown upon mechanical grinding using spatula or pestle (Fig. 5). Fig. 5a shows dramatic change in UV-vis-NIR absorption spectra of **2** in the solid state. A drop-cast film of **2** deposited from a dichloromethane solution showed absorption bands only in the visible region. After grinding the film of **2**, however, distinct and broad absorption bands in the NIR region were appeared at 970 nm. A drop of dichloromethane to brown powders of **2** recovered the original yellow colour and the NIR absorption bands disappeared.

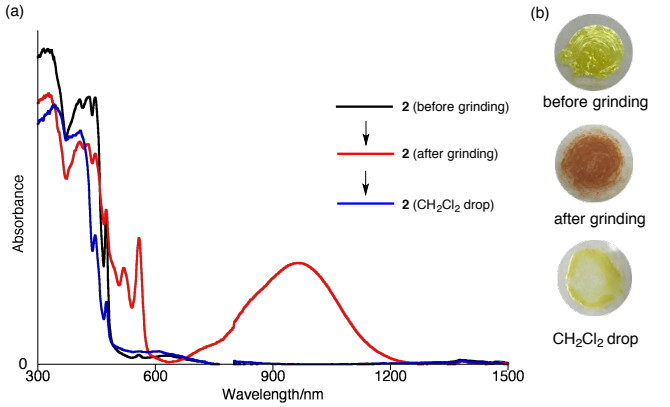

Fig. 5 (a) Solid-state UV-vis-NIR absorption spectra of a drop-cast film of **2** before and after grinding by spatula along with the spectrum of the sample after one drop of CH_2Cl_2. The baselines of all spectra were corrected. (b) Photographs of solid color of **2** before and after grinding.

Compounds containing long carbon–carbon single bonds often undergo C–C bond dissociation by external stimuli such as heating, pressing and grinding.[10b] The C–C bond between dicyanomethyl units are predisposed to cleavage to afford dicyanomethyl radical species.[12] Further analysis of the chromic behaviour of **2** was performed by ESR measurement. While almost no ESR signals were detected before grinding, clear ESR signals (g = 2.0026) were observed in the brown sample of **2** after grinding (Fig. 6a). The content percentage of the radical species in the sample was estimated by ESR signal intensities, indicating the presence of 2.4% of the radical

species in the sample after grinding, whereas the amount of the radical was only 0.16% in the as-prepared sample of **2**. This result clearly suggests the generation of radical species by grinding. The ESR signal remained unchanged for a prolonged time (4 months) at room temperature under air, indicating the high stability of radical species in the solid state (Fig. S18). Spin density of corresponding monoradical **1**$^{\bullet}$ calculated by the DFT method delocalised on the HBC skeleton and dicyanomethyl unit (Fig. 5b). The calculated absorption peak of corresponding monoradical **1**$^{\bullet}$ by the TD-DFT method was in good agreement with the new NIR peak after grinding (Fig. 6). According to the fact that no bond dissociation was observed on heating of **2** in the solution state (Fig. S15), the bond dissociation on grinding is originated by mechanical stimuli.

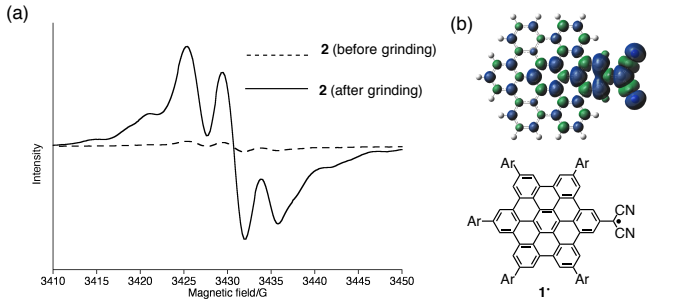

Fig. 6 (a) ESR spectra of **2** before and after grinding of its powder sample. (b) Calculated spin distribution of monoradical **1**$^{\bullet}$.

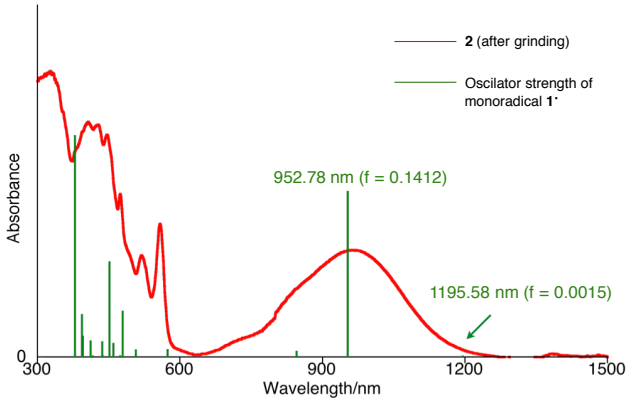

Fig. 7 Calculated absorption spectrum of monoradical **1**$^{\bullet}$ by the TD-DFT method.

Cyclic HBC trimer **6** also exhibited a similar mechanochromic behaviour. An as-prepared sample of **6** was yellow, which turned to brown after grinding. In solid-state UV-vis-NIR absorption spectra of **6**, the ground sample exhibited a NIR absorption band, which disappeared by a drop of dichloromethane (Fig. 8). ESR measurement also revealed the formation of radical specie by mechanical grinding (Fig. S19).

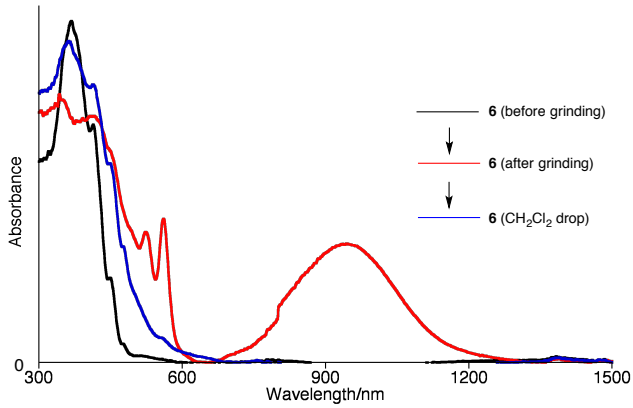

Fig. 8 (a) Solid-state UV-vis-NIR absorption spectra of a drop-cast film of **6** before and after grinding along with the spectrum of the sample after one drop of CH_2Cl_2. The baselines of all spectra were corrected.

Conclusions

In conclusion, the synthesis of tetracyanoethylene-bridged HBC dimer **2** and trimer **6** were accomplished efficiently through simple oxidation of dicyanomethyl-substituted HBCs **1** and **5**. These HBC oligomers exhibited NIR mechanochromic behaviour. ESR measurement revealed the generation of persistent radical species for a prolonged period upon grinding, indicating high stability of the radical. The mechanochromic properties with NIR absorption and the long-lived coloured state (more than four months) would be useful in applications in the field optoelectronics, such as switching devices and molecular memory devices. The present results demonstrate that introduction of dicyanomethyl units to PAHs renders stimuli-responsive features to functional π-systems.

Acknowledgements

We acknowledged Prof. Taishi Takenobu and Dr. Hisaaki Tanaka at Nagoya University for ESR measurement. This work was supported by a Grant-in-Aid for Scientific Research on Innovative Areas “New Polymeric Materials Based on Element-Blocks (No.2401)” (JSPS KAKENHI Grant Number 15H00731) and “pi-System Figuration” (No.2601) (JSPS KAKENHI Grant Number JP26102003) and a Grant-in-Aid for Encouragement of Young Scientists (A) (No. 16H06031). S.H. also acknowledges the Asahi Glass Foundation and TOBEMAKI Scholarship Foundation for financial support. K.O. appreciates the JSPS Research Fellowship for Young Scientists.

Experimental Section

Synthesis and Characterisation

2,5-Bis(dicyanomethyl)-8,11,14,17-tetramesitylhexabenzo[*bc*,*ef*,*hi*,*kl*,*no*,*qr*]coronene 5. A Schlenk flask containing NaO^{t}Bu (97.4 mg, 1.01 mmol) and malononitrile (50.6 mg, 0.766 mmol) was purged with N_2, and then charged with anhydrous and degassed THF (13 mL), and then the resulting

mixture was stirred for 15 min at room temperature. To the mixture was added **4** (158.6 mg, 0.127 mmol), tetrakis(triphenylphosphine)palladium (45.2 mg, 0.039 mmol) and copper(I) iodide (48.6 mg, 0.255 mmol) at room temperature. After stirred at 60 °C for 12 h, the reaction mixture was quenched with aqueous HCl, extracted with CH_2Cl_2, and then dried over Na_2SO_4. The solvent was removed in vacuo, and purification of the residue by GPC ($CHCl_3$) followed by recrystallisation from $CHCl_3$/MeOH afforded **5** (96.8 mg, 0.0862 mmol) in 68% yield. ^{1}H NMR ($CDCl_3$): δ 9.34 (s, 2H, HBC), 9.27 (s, 2H, HBC), 9.12 (s, 2H, HBC), 9.09 (s, 2H, HBC), 9.06 (s, 2H, HBC), 9.05 (s, 2H, HBC), 7.15 (s, 4H, Mes), 7.08 (s, 4H, Mes), 5.71 (s, 1H, $CH(CN)_2$), 2.42–2.46 (s+s, 12H, *p*-Me), 2.22–2.25 (s+s, 24H, *o*-Me) ppm; ^{13}C NMR ($CDCl_3$): δ 141.1, 138.8, 138.6, 137.8, 137.6, 136.3, 136.1, 132.8, 131.3, 131.3, 131.2, 131.0, 129.6, 128.7, 128.7, 127.0, 125.2, 124.7, 124.3, 124.1, 123.9, 122.5, 121.9, 121.6, 120.6, 120.5, 112.0, 29.3, 21.5, 21.5, 21.4, 21.3 ppm; HR-MS (ESI-MS): *m/z* = 1123.4794, calcd for $(C_{84}H_{59}N_4)^+$ = 1123.4740 $[(M + H)^+]$; UV/vis (CH_2Cl_2): λ_{max} (ε [M^{-1} cm^{-1}]) = 347 (72000), 363 (170000), 445 (3700) nm.

Synthesis of tetracyanoethylene-bridged HBC trimer 6. A Schlenk flask containing **5** (56.19 mg, 50.0 μmol) and PbO_2 (604.0 mg, 2.53 mmol) was purged with N_2, and then charged with anhydrous and degassed CH_2Cl_2 (3.0 mL). The resulting mixture was stirred for 4 h at room temperature. The reaction mixture was filtered through Celite with CH_2Cl_2, concentrated in vacuo. Purification of the residue by column chromatography on silica-gel (CH_2Cl_2/EtOAc = 50:1 as an eluent) followed by recrystallisation from CH_2Cl_2/MeOH afforded **6** (43.81 mg, 13.0 μmol) in 78% yield. ^{1}H NMR (tetrachloroethane-d_2, 26 °C): δ 10.37 (s, 6H, HBC), 10.12 (s, 6H, HBC), 9.57 (s, 6H, HBC), 9.29 (s, 6H, HBC), 9.19 (s, 12H, HBC), 7.27 (s, 12H, Mes), 7.14 (s, 12H, Mes), 2.29–2.59 (m, Me) ppm; ^{13}C NMR (tetrachloroethane-d_2, 26 °C): δ 141.13, 140.74, 140.60, 138.52, 138.41, 137.26, 137.15, 136.61, 135.97, 135.84, 132.68, 131.09, 130.98, 130.89, 130.82, 129.36, 128.87, 128.42, 128.23, 126.22, 124.50, 124.35, 124.19, 123.98, 123.82, 123.47, 122.75, 122.29, 122.12, 121.81, 120.28, 110.68, 55.81, 21.51, 21.42, 21.33, 21.20 ppm; HR-MS (ESI-MS): *m/z* = 3386.3363, calcd for $(C_{252}H_{168}N_{12}Na)^+$ = 3386.3473 $[(M + Na)^+]$; UV/vis (CH_2Cl_2): λ_{max} (ε [M^{-1} cm^{-1}]) = 370 (360000), 413 (126000), 445 (24600) nm.

Notes and references

1 (a) P. Rajamalli, P. Gandeepan, M. J. Huang and C. H. Cheng, *J. Mater. Chem. C* 2015, **3**, 3329-3335; (b) K. Imato, M. Nishihara, T. Kanehara, Y. Amamoto, A. Takahara and H. Otsuka, *Angew. Chem. Int. Ed.* 2012, **51**, 1138-1142; (c) Y. Sagara, T. Kato, *Nat. Chem.* 2009, **1**, 605-610; (d) P. C. Xue, J. P. Ding, P. P. Wang and R. Lu, *J. Mater. Chem. C* 2016, **4**, 6688-6706.

2 (a) K. Nagura, S. Saito, H. Yusa, H. Yamawaki, H. Fujihisa, H. Sato, Y. Shimoikeda and S. Yamaguchi, *J. Am. Chem. Soc.* 2013, **135**, 10322-10325; (b) J. Kunzelman, M. Kinami, B. R. Crenshaw, J. D. Protasiewicz and C. Weder, *Adv. Mater.* 2008, **20**, 119-122.

3 (a) M. J. Robb, T. A. Kim, A. J. Halmes, S. R. White, N. R. Sottos, J. S. Moore, *J. Am. Chem. Soc.* 2016, **138**, 12328-12331; (b) K. Imato, T. Kanehara, S. Nojima, T. Ohishi, Y. Higaki, A. Takahara, H. Otsuka, *Chem. Commun.* 2016, **52**, 10482-10485.

4 (a) X. Zhang, Z. Chi, Y. Zhang, S. Liu and J. Xu, J. Mater. Chem. C, 2013, **1**, 3376-3390; (b) Z. Chi, X. Zhang, B. Xu, X. Zhou, C. Ma, Y. Zhang, S. Liu and J. Xu, *Chem. Soc. Rev.* 2012, **41**, 3878-3896.

5 (a) M. M. Caruso, D. A. Davis, Q. Shen, S. A. Odom, N. R. Sottos, S. R. White and J. S. Moore, *Chem. Rev.* 2009, **109**, 5755-5798; (b) M. D. Molin, Q. Verolet, A. Colom, R. Letrun, E. Derivery, M. Gonzalez-Gaitan, E. Vauthey, A. Roux, N. Sakai and S. Matile, *J. Am. Chem. Soc.* 2015, **137**, 568-571; (c) M. D. Molin, Q. Verolet, S. Soleimanpoura and S. Matile, *Chem. Eur. J.* 2015, **21**, 6012-6021; (d) Y. Wang, X. Tan, Y.-M. Zhang, S. Zhu, I. Zhang, B. Yu, K. Wang, B. Yang, M. Li, B. Zou and S. X.-A. Zhang, *J. Am. Chem. Soc.* 2015, **137**, 931-939.

6 Y. Q. Dong, J. W. Y. Lam and B. Z. Tang, *J. Phys. Chem. Lett.* 2015, **6**, 3429-3436.

7 H. Ito, M. Muromoto, S. Kurenuma, S. Ishizaka, N. Kitamura, H. Sato and T. Seki, *Nat. Commun.* 2013, **4**, 2009.

8 M. Okazaki, Y. Takeda, P. Data, P. Pander, H. Higginbotham, A. P. Monkman and S. Minakata, *Chem. Sci.* 2017, *in press* (doi: 10.1039/C6SC04863C).

9 S. Yagai, S. Okamura, Y. Nakano, M. Yamauchi, K. Kishikawa, T. Karatsu, A. Kitamura, A. Ueno, D. Kuzuhara, H. Yamada, T. Seki and H. Ito, *Nat. Commun.* 2014, **5**, 4013.

10 (a) A. R. de Luzuriaga, J. M. Matxain, F. Ruipérez, R. Martin, J. M. Asua, G. Cabañero and I. Odriozola, *J. Mater. Chem. C* 2016, **4**, 6220-6223; (b) Y. Mori, N. Yamada, M. Kanazawa, Y. Horikoshi, Y. Watanabe and K. Maeda, *Bull. Chem. Soc. Jpn.* 1996, **69**, 2355-2359.

11 M. Frenette, C. Aliaga, E. Font-Sanchis and J. C. Scaiano, *Org. Lett.* 2004, **6**, 2579-2582.

12 T. Kobashi, D. Sakamaki and S. Seki, *Angew. Chem. Int. Ed.* 2016, **55**, 8634-8638.

13 H. D. Hartzler, *J. Org. Chem.* 1966, **31**, 2654-2658.

14 (a) T. Aida, E. W. Meijer and S. I. Stupp, *Science* 2012, **335**, 813-817; (b) W. Pisula, X. Feng and K. Müllen, *Adv. Mater.* 2010, **22**, 3634-3649.

15 R. Yamaguchi, S. Ito, B. S. Lee, S. Hiroto, D. Kim and H. Shinokubo, *Chem. Asian J.* 2013, **8**, 178-190.

16 (a) K. Hemelsoet, V. V. Speybroeck, M. Waroquier, *J. Phys. Chem. A* 2008, **112**, 13566-13573; (b) K. Hemelsoet, V. V. Speybroeck and M. Waroquier, *ChemPhysChem.* 2008, **9**, 2349-2358.

17 K. Oda, S. Hiroto, I. Hisaki and H. Shinokubo, *Org. Biomol. Chem.* 2017, **15,** 1426-1434.

18 Crystallographic data for **2**: $C_{180}H_{131}N_4$, *M*w = 2349.89, triclinic, *P*-1, *a* = 22.5096(6) Å, *b* = 23.7690(6) Å, *c* = 33.7136(6) Å, α = 95.064(2)°, β = 98.276(2)°, γ = 110.727(2)°, *Z* = 4, *R* = 0.0967 (*I* > 2.0 σ (*I*)), *R*w = 0.2915 (all data), GOF = 0.970; crystallographic data for **2** has been deposited with the Cambridge Crystallographic Data Centre as supplementary publication no. CCDC 1537349.

19 S. R. Chaudhari and N. Suryaprakash, *J. Mol. Struct.* 2012, **1017**, 106-108.